RESEARCH ARTICLE

Metabolic alteration of HepG2 in scaffold-based 3-D culture: Proteomic approach

Dumnoensun Pruksakorn[1], Kriengsak Lirdprapamongkol[2], Daranee Chokchaichamnankit[2], Pantipa Subhasitanont[2], Khajeelak Chiablaem[2], Jisnuson Svasti[1,2,3,4], and Chantragan Srisomsap[2]

[1] Applied Biological Sciences Program, Chulabhorn Graduate Institute, Bangkok, Thailand
[2] Laboratory of Biochemistry, Chulabhorn Research Institute, Bangkok, Thailand
[3] Department of Biochemistry and Center for Protein Structure and Function, Faculty of Science, Mahidol University, Bangkok, Thailand
[4] Center of Excellence on Environmental Health, Toxicology and Management of Chemicals, Bangkok, Thailand

Received: March 4, 2010
Revised: August 17, 2010
Accepted: August 22, 2010

3-D cell culture models are important in cancer biology since they provide improved understanding of tumor microenvironment. We have established a 3-D culture model using HepG2 in natural collagen-based scaffold to mimic the development of small avascular tumor *in vivo*. Morphological characterization showed that HepG2 colonies grew within the interior of the scaffold and showed enhanced extracellular matrix deposition. High levels of cell proliferation in the outermost regions of the scaffold created a hypoxic microenvironment in the 3-D culture system, as indicated by hypoxia-inducible factor-1α stabilization, detectable by Western blotting and immunohistochemistry. Proteomic studies showed decreased expression of several mitochondrial proteins and increased expression of proteins in anaerobic glycolysis under 3-D culture compared to monolayer culture. Creatine kinase was also upregulated in 3-D culture, indicating its possible role as an important energy buffer system under hypoxic microenvironment. Increased levels of proteins in nucleotide metabolism may relate to cellular energy. Thus, our results suggest that HepG2 cells under 3-D culture adapt their energy metabolism in response to hypoxic conditions. Metabolic alterations in the 3-D culture model may relate to physiological changes relevant to development of small avascular tumor *in vivo* and their study may improve future therapeutic strategies.

Keywords:
3-D culture / Cell biology / Creatine kinase / HepG2 / Hypoxia

1 Introduction

The etiology and pathophysiology of hepatocellular carcinoma (HCC) are well defined. Although surgical resection or percutaneous intervention is often useful initially, the tumor can recur. Moreover, there is still insufficient evidence to show whether adjuvant or neo-adjuvant chemotherapies can increase survival in long-term follow-up. Therefore, prevention of recurrent secondary HCC after the initial operation is an important area of research [1]. Thus, a study model, providing better information about the microenvironment of small avascular tumor, would be useful for understanding tumorigenesis and the natural history of the recurrent lesion.

The microenvironment of the tumor is considered to play a pivotal role in the regulation of cellular phenotype and function [2, 3]. The 3-D culture model can improve understanding of tumorigenesis by providing a more realistic microenvironment, which is more similar to that of small

Correspondence: Dr. Chantragan Srisomsap, Laboratory of Biochemistry, Chulabhorn Research Institute, Vibhavadee-Rangsit Road, Laksi, Bangkok 10210, Thailand
E-mail: chantragan@cri.or.th
Fax: +66-2-5742027

Abbreviations: CK/PCr, creatine kinase/phosphocreatine; **DAB,** diaminobenzidine; **HCC,** hepatocellular carcinoma; **HIF-1α,** hypoxia-inducible factor 1α; **MTT,** 3-4,5-dimethylthiazol-2-yl-2,5-diphenyltetrazolium bromide; **NAD$^+$,** nicotinamide adenine dinucleotide; **SEM,** scanning electron microscope

avascular tumors than monolayer culture. Thus, 3-D culture is an important intermediate between conventional monolayer culture and *in vivo* experimentation [4]. Several techniques have been used for 3-D tumor culture, including scaffold-based, spheroid aggregation, liquid overlay, microcarrier beads and rotary cell culture system. Recently, the HepG2 cell line under 3-D culture by spheroid aggregation showed upregulated expression of liver-specific proteins, such as albumin, compared to monolayer culture; this is more similar to HCC *in vivo* [5]. More recently, a HCC cell line (HAb18G/CD147) under 3-D culture with liquid overlay technique showed increased invasive and metastatic potential by enhancing expression and activation of focal adhesion kinases, and increasing production of matrix metalloproteinase [6]. 3-D culture using scaffold-based techniques offers advantages in providing a structural support for cellular attachment with a different orientation. Scaffold architecture and materials may also modify responses of cells. Furthermore, the scaffold technique has a potential for studying chemical delivery devices, vascularization and tissue development [7].

Proteomics has been used to explore global protein change in 3-D culture compared with the conventional monolayer culture in cancers such as colon carcinoma, neuroblastoma and ovarian cancer [4, 8, 9]. However, proteomic study of the HCC cell line in 3-D culture is still lacking. Here, 3-D culture of HepG2 was established using a natural collagen-based scaffold and characterized morphologically. Protein expression was studied in 3-D culture compared to the conventional monolayer culture using 2-DE and ESI-MS/MS. Significant protein changes were analyzed and a hypothetical network was constructed of physiological changes under the 3-D microenvironment.

2 Materials and methods

2.1 Monolayer and 3-D cell culture

Human HCC cells (HepG2) were maintained in DMEM at 37°C in a humidified atmosphere of 5% CO_2. For 3-D culture, natural collagen material from bovine hide, Lyostypt® (B. Braun, Germany), with collagen type I as a major component, was used as a scaffold [10]. The scaffold was sterilized with 70% ethanol, washed with PBS and then squeezed using a pipette tip, while removing PBS, so the scaffold shrunk to dryness. Forty microliters of cell suspension (1×10^6 cell/mL) was seeded into the shrunken scaffold, followed by 2 h incubation to allow cell adhesion. Culture media (200 μL) was gently poured to cover all pieces of scaffold. Cell-seeded scaffold was incubated overnight. Then 1 mL culture media was added and the culture media was changed on alternate days [10–12].

2.2 Proliferative rate, metabolic rate and creatine kinase activity

Cell number was estimated by DNA quantification using PicoGreen (Invitrogen, USA). Cells were washed twice with PBS and stored in 100 μL TE buffer (0.2% Triton X-100, 10 mM Tris, pH 7.0, 1 mM EDTA). Samples were repeatedly frozen and thawed three times and DNA was quantified by a fluorescence microplate reader, with excitation and emission wavelengths of 485 and 520 nm, respectively [13].

Metabolic activity was analyzed using MTT (3-4,5-dimethylthiazol-2-yl-2,5-diphenyltetrazolium bromide) assay. Cells were incubated in 200 μL media containing MTT (0.5 mg/mL) at 37°C for 2 h. MTT-formazan crystals were dissolved in 200 μL DMSO and absorbance was measured at 550 and 650 nm (as reference wavelength) in a microplate reader [14].

Creatine kinase (CK) activity was measured using Enzy-Chrome™ CK Assay Kit (BioAssay Systems, USA) [15]. Samples were frozen at −80°C, thawed and the supernatants were immediately used for CK assay. Activity was normalized to total protein and all experiments were performed in triplicate. Data are expressed as mean ± SD and analyzed by Student *t*-test, *p*-value <0.05 being considered significant.

2.3 Histological and morphological studies

Cell-seeded scaffolds were placed in 10% neutral buffered formalin until analysis. Specimens were dehydrated and embedded in paraffin at 60°C. Histological sections were stained with HE and Alcian Blue for microscopic analysis. For morphology evaluation, specimens were observed under a scanning electron microscope (SEM).

2.4 Protein extraction

For monolayer cell culture, cells at 90% confluency were washed with PBS, scraped in 5 mL of 0.25 M sucrose containing protease inhibitor cocktail 1:500 (Sigma, USA) and spun down. Samples were resuspended in lysis buffer, sonicated and centrifuged [16]. For 3-D culture, cells at 90% confluency were rinsed with 0.25 M sucrose five times to remove culture media. Lysis buffer was added and samples were gently homogenized, sonicated and centrifuged. After precipitation with trichloroacetic acid, the protein pellet was dried and kept at −80°C until use. Protein pellets were resuspended in lysis buffer and protein content determined using the Bradford assay [17].

2.5 2-D PAGE and image analysis

Immobiline™ Drystrips, 13 cm, nonlinear, pH 3–10 gradient, IPG gel strips (Bio-sciences AB, Sweden) were

incubated overnight with 450 μg protein. IEF was performed at 6500 V/h, 55 μA *per* gel strip using an Ettan IPGphor 3 (GE Healthcare). For the second-dimension SDS-PAGE, the IPG strips were equilibrated in equilibration buffer in two steps. Electrophoresis was performed in a SE 600 Ruby apparatus (Amersham Bioscience, USA) at 25 mA, followed by Coomassie blue R-250 staining. Gels were scanned using Labscan 5.0 and analyzed by the ImageMaster 2D Platinum 6.0 program [16]. 2-DE was independently performed and compared in triplicate and consistent spots were reported for statistical analysis, paired *t*-test was performed to compare data from three repeat experiments. Only spots that showed consistently significant differences ($\pm$over twofold, $p<0.05$) were selected for MS analysis.

2.6 In-gel digestion

Spots, showing more than twofold change, were excised and transferred to 0.5 mL microfuge tubes and in-gel digestion was performed [16]. Following dye removal, reduction with 10 mM DTT and alkylation with 100 mM iodoacetamide were performed. After removing reagents, gel pieces were dried. Fifty microliters of digestion buffer and 0.1 μg of trypsin (Promega, USA) were added, followed by incubation at 37°C overnight and collection of digestion buffer.

2.7 Protein identification

LC-MS/MS analysis was performed using a capillary LC system (Waters) coupled to a Q-TOF mass spectrometer (Micromass, UK) equipped with Z-spray ion-source working in nanoelectrospray mode. Glu-fibrinopeptide was used to calibrate the instrument in MS/MS mode. Tryptic peptides were concentrated and desalted on a 75 μm id × 150 mm C_{18} PepMap column (LC Packing, Netherlands). Eluents A and B were 0.1% formic acid in 97% water, 3% ACN and 0.1% formic acid in 97% ACN, respectively. Sample (6 μL) was injected into the nano-LC and separation was performed using the gradient: 0 min 7% B, 35 min 50% B, 45 min 89% B, 49 min 80% B, 50 min 7% B and 60 min 7% B. For ESI-Q-TOF analysis, automatic scan rate was 1.0 s with interscan delay of 0.1 s. Parent mass peaks with range from 400 to 1600 *m/z* were selected for MS/MS analysis. Collision energy was fixed at 38 eV. MS/MS data were processed using MassLynx 4.0 software (Micromass) and converted to PKL files by the ProteinLynx 2.2 software (Waters), which were then analyzed using the MASCOT search engine (http://www.matrixscience.com). Search parameters were defined as follows: Database, Swiss-Prot; taxonomy, *Homo sapiens*; enzyme, trypsin; one missed cleavage allowed. Peptide and fragment mass tolerance were set at 1.2 and 0.6 Da, respectively. Proteins with molecular weight and p*I* consistent with gel region, with at least one peptide exceeding score threshold ($p<0.05$), were considered positively identified [16].

2.8 Western blot analysis

Proteins were subjected to 7.5% SDS-PAGE and electrophoretically transferred to nitrocellulose membranes (Amersham, UK). The membrane was probed with hypoxia-inducible factor 1α (HIF-1α) antibody (Santa Cruz, USA), 1:500 diluted, overnight, followed by 1:2000 anti-rabbit secondary antibody (DakoCytomation, Denmark) for 1 h. Bands were detected using the ECL plus detection system (Amersham, UK).

2.9 Immunohistochemistry

Formalin-fixed, paraffin-embedded tissue sections (3 μM) were mounted on positively charged slides and baked overnight at 60°C. HepG2 cells in 3-D culture were immunostained with HIF-1α antibody (Santa Cruz), dilution 1:25, using a Ventana Benchmark XT auto-immunostainer (Tucson, AZ, USA) with ultraView™ Universal DAB Detection Kit (Ventana, USA). Slides were counterstained with hematoxylin.

3 Results

3.1 Growth pattern in 3-D and monolayer culture

Growth of HepG2 in 3-D culture and monolayer culture was studied using MTT assay for determining metabolic activity and PicoGreen® to assay double-strand DNA. Both assays showed differences in growth pattern between 3-D and monolayer cultures (Fig. 1A). HepG2 in monolayer culture showed rapid growth but decreased in number after maximal growth at day 7. However, HepG2 in 3-D culture had slower growth but remained at stationary phase longer up to 13 days.

3.2 Histology and morphology of HepG2

3-D culture of HepG2 was characterized by low-power and high-power light microscopy and by SEM. In gross appearance (Fig. 1B, left column), black spots in the scaffold represent cells or colonies stained with MTT. Progressive growth of HepG2 colonies was visible through the bulky material. Histological analysis (Fig. 1B, middle column) showed collagen fibers in pink, with nuclei and cytoplasm in deep blue and faint pink (shown with pointer), respectively. HepG2 cells were distributed throughout the scaffold at day 2 after first seeded. Then some colonies in the inner scaffold become enlarged with loose intercellular spacing from day 2 to day 6. Later, colonies grew more at the scaffold surface

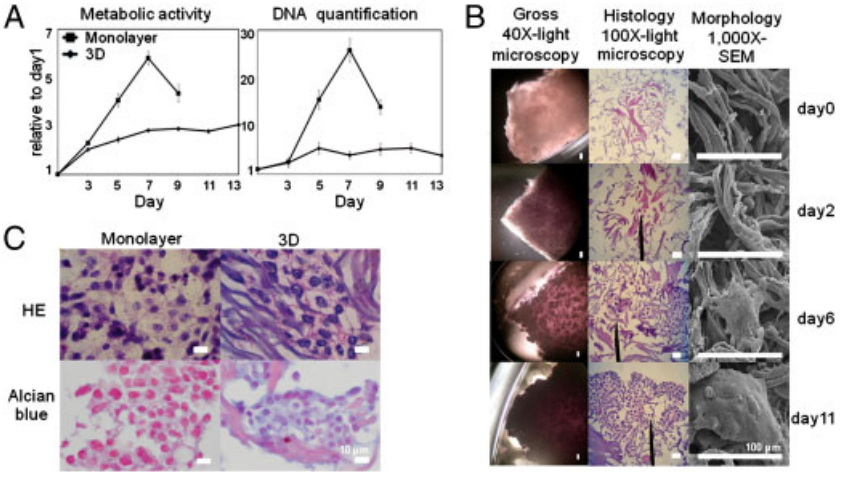

Figure 1. Characterization of 3-D culture model. (A) Growth pattern of HepG2 in monolayer culture (square) and 3-D culture (circle) relative to day 1, determined by metabolic activity and DNA quantification. (B) Morphology and histology of HepG2 in collagen-based scaffold by light microscopy and SEM (scale bars, 100 μm). Left column shows gross appearance under low-power field light microscope; middle column shows cross-sectional histology stained with HE; right column shows morphology of collagen-based 3-D culture under SEM. Rows show results on different days, from day 0 (scaffold alone), day 2, day 6 and day 11 in the first, second, third and fourth rows, respectively. (C) High power field histology of both culture systems at day 6 stained with HE and Alcian blue (scale bars, 10 μm).

from day 6 to day 11. Histological results at days 2, 6 and 11 are also shown at different magnifications in the Supporting Information.

SEM (Fig. 1B, right column) showed the morphology of HepG2 colonies with extracellular material covering the collagen fibers at day 6 and day 11 in agreement with light microscopy.

In high power histology with HE staining, cell–cell contacts were observed in monolayer culture, but intercellular spaces were observed between cell colonies in 3-D culture at day 6. Alcian blue staining showed positive results (faint blue) in 3-D culture indicating sulfated-glycosaminoglycan deposition, but no staining was observed in monolayer culture.

3.3 Comparison of 2-DE profiles between 3-D and monolayer cultures

Protein expression of HepG2 cells in 3-D culture and in monolayer culture was compared in three separate experiments. Spots were identified after automatic spot detection, background and contamination removal and volume normalization. Representative 2-DE maps of 3-D and monolayer culture are shown in Fig. 2A, with complete information of significantly different spots shown as Supporting Information (Table 1S). In total, 823 ± 45 spots were found in monolayer culture and 762 ± 65 spots were found in 3-D culture. Comparisons showed that 526 spots were consistently matched between 3-D culture and monolayer culture in three repetitions. Marked statistically different changes (more than twofold change with $p < 0.05$) were found in 73 spots. Nine spots were uniquely present in monolayer culture including heat-shock 70 kDa protein 9B, lamin A/C, liver carboxylesterase, glutamate dehydrogenase 2, long-chain-fatty-acid-CoA ligase 3, pyruvate dehydrogenase, laminin receptor1, isovaleryl-CoA dehydrogenase and heterogenous nuclear ribonucleoprotein C. Conversely, three spots were uniquely present in 3-D culture namely fibronectin, annexinVII and inosine triphosphate pyrophosphatase. Some spots (a–e) in 3-D culture were derived from FBS, due to contamination resulting from incomplete removal of FBS by washing.

3.4 Anaerobic glycolysis and HIF-1α stabilization in 3-D culture

The expanded region of Fig. 2A shows selected areas of 2-DE gels with three important anaerobic glycolytic enzymes, 2-phosphopyruvate hydratase (spot no.30), phosphoglycerate kinase1 (spot no.36) and triosephosphate isomerase (spot no.69), being increased in 3-D culture compared to monolayer culture. Stabilization of HIF-1α protein in 3-D culture was observed by immunoblotting (Fig. 2B), compared with HepG2 treated with $CoCl_2$, a HIF-1α stabilizing agent, as positive control. Positive immunohistochemical staining of HIF-1α was also observed in 3-D culture (Fig. 2B).

Proteins showing significantly different expression were classified into four major groups (Fig. 3): cellular respiration proteins (Fig. 3A and B), nucleotide metabolism proteins (Fig. 3C), cytoskeletal/cytoskeletal organization and related proteins (Fig. 3D) and iron metabolism proteins (Fig. 3E).

For cellular respiration, 3-D culture showed down-regulation of several mitochondrial proteins involved in

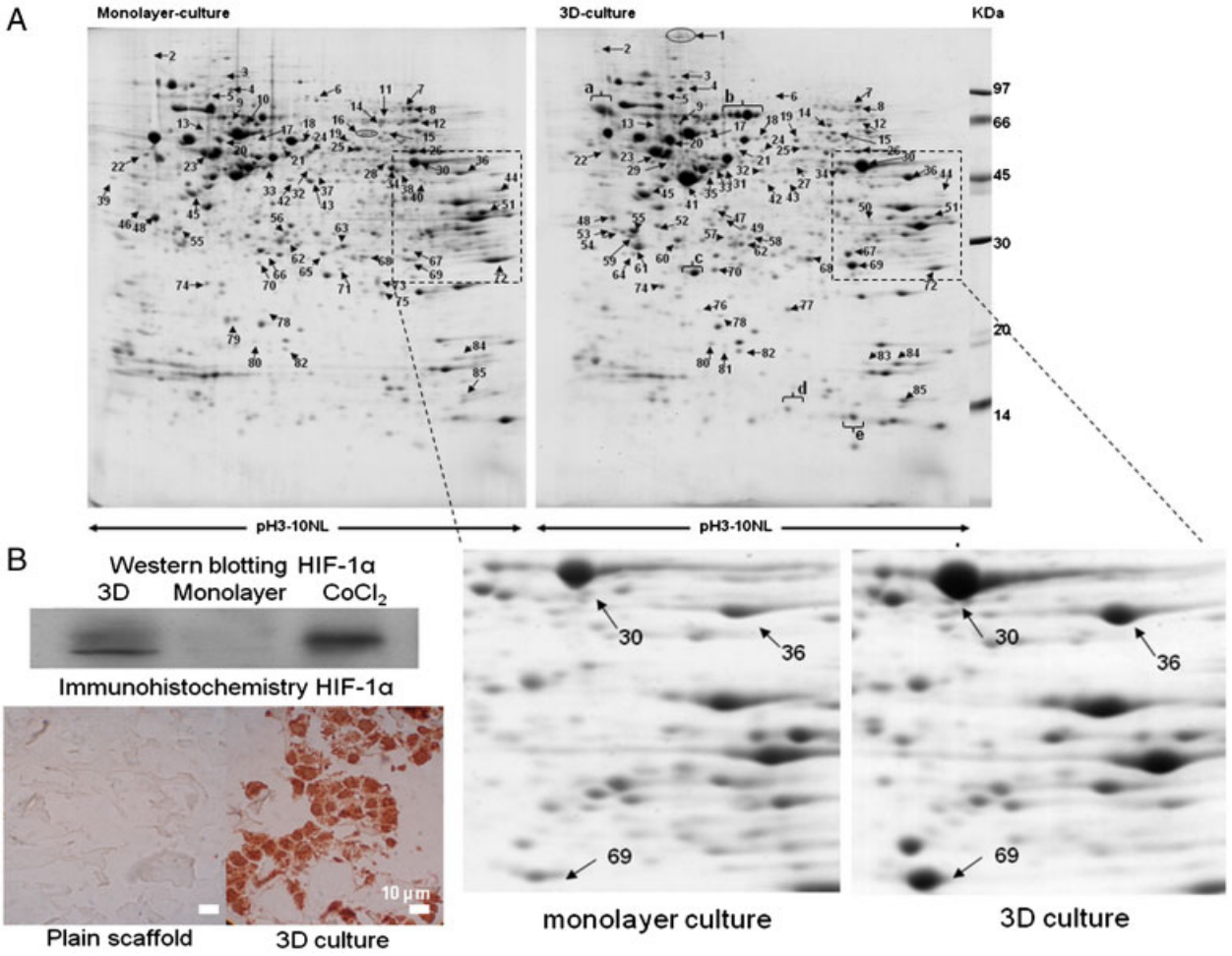

Figure 2. Protein expression by HepG2 cells in 3-D and monolayer culture. (A) 2-DE patterns of total proteins separated on pH 3–10 nonlinear IPG strips and 12.5% SDS-PAGE, followed by CBB staining. Expanded region shows some proteins involved in anaerobic glycolysis. Label on 2-DE of 3-D culture represent spots contaminating from FBS (a) α1-anti-chymotrypsin, (b) serum albumin, (c) apolipoprotein A1, (d–e) hemoglobin. (B) Western blot detection of HIF-1α stabilization with equal protein loading and positive immunohistochemistry of HIF-1α of HepG2 in 3-D culture (scale bars, 10 μm).

oxidative phosphorylation, electron transport and redox regulation (Fig. 3A). Decrease in expression of pyruvate dehydrogenase would lead to reduction of pyruvate conversion to acetyl-CoA for the Kreb's cycle, while decreased expression of phosphoenolpyruvate carboxykinase would decrease conversion of pyruvate to glucose-6P by gluconeogenesis. Decreased expression of fatty acid metabolism-related enzymes, enoyl Co-A hydratase, acyl Co-A dehydrogenase, isovaleryl Co-A dehydrogenase, and fatty acid Co-A ligase 3, indicate that fatty acid oxidation was also reduced. Moreover, decreased expression of electron transport, redox regulation and other proteins in the mitochondria including NADH dehydrogenase, ubiquinol-cytochrome-c reductase, mitochondrial inner membrane protein, thioredoxin, elongation factor Tu, glutamate dehydrogenase and aldehyde dehydrogenase indicate overall reduction of mitochondrial function in 3-D culture. However, upregulation of several important anaerobic glycolytic enzymes including triosphosphate isomerase, phosphoglycerate mutase1, phosphoglycerate kinase1, 2-phosphopyruvate hydratase (Fig. 3B) suggest increased anaerobic glycolysis in 3-D culture.

3.5 Changed expression of proteins in nucleotide metabolism, cytoskeleton and iron metabolism

3-D culture showed increased expression of nucleotide metabolism proteins, including IMP cyclohydratase, inosine triphosphopyrophosphatase involved in *de novo* purine biosynthesis, adenine phosphoribosyltransferase involved in salvage purine biosynthesis and uridine/cytidine monophosphate kinase involved in pyrimidine biosynthesis (Fig. 3C). Expression of cellular cytoskeletal mass and

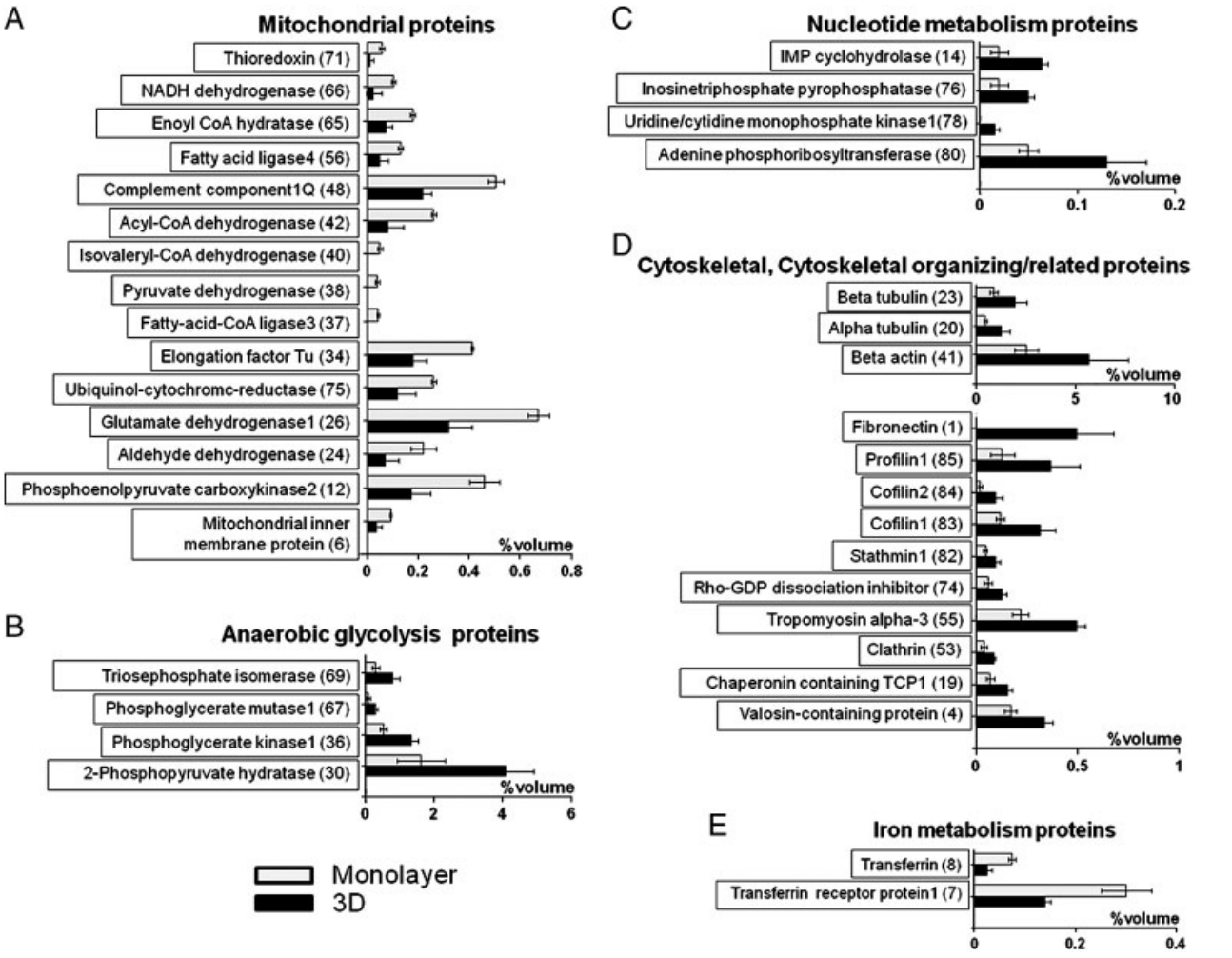

Figure 3. Protein expression of HepG2 showing four major groups of proteins significantly changed. Cellular respiration proteins include (A) mitochondrial and (B) anaerobic glycolysis proteins; (C) Nucleotide metabolism proteins; (D) Cytoskeletal/cytoskeletal organizing and related proteins; (E) Iron metabolism proteins. Black bar shows 3-D culture and gray bar shows monolayer culture. Spot numbers, as referred to in Fig. 2 and Supporting Information Table 1S, are shown in brackets.

cytoskeletal organizing proteins was increased in 3-D culture including: actin, tubulin, tropomyosin, cofilin, profilin, stathmin, rho-GDP dissociation inhibitor and chaperonin containing TCP1. Furthermore, expression of baso-apical polarizing related proteins; clathrin and valosin-containing protein was also increased (Fig. 3D). Expression of iron metabolism proteins, transferrin and transferrin receptor protein was decreased (Fig. 3E). Identification data are shown in Supporting Information (Table 1S).

3.6 Increased expression of CK

Expression of CK B, known as an energy buffer system in some normal tissues, was significantly increased in 3-D compared to monolayer culture (Fig. 4A). Enzymatic activity of CK in the two culture systems (Fig. 4B) also showed a similar change, increasing between day 2 and day 5 and decreasing thereafter. However, 3-D culture showed significantly higher CK activity than monolayer culture on days 3, 5, 6 and 7.

4 Discussion

In this study, 3-D culture of HepG2 was established to produce some characteristics representative of small avascular tumors *in vivo* before the onset of angiogenesis. HepG2 in 3-D culture showed a period of hypoxic microenvironment with stabilization of HIF-1α. Proteomic profiles of HepG2 provided an overview of differences in cellular metabolism between 3-D culture and monolayer culture.

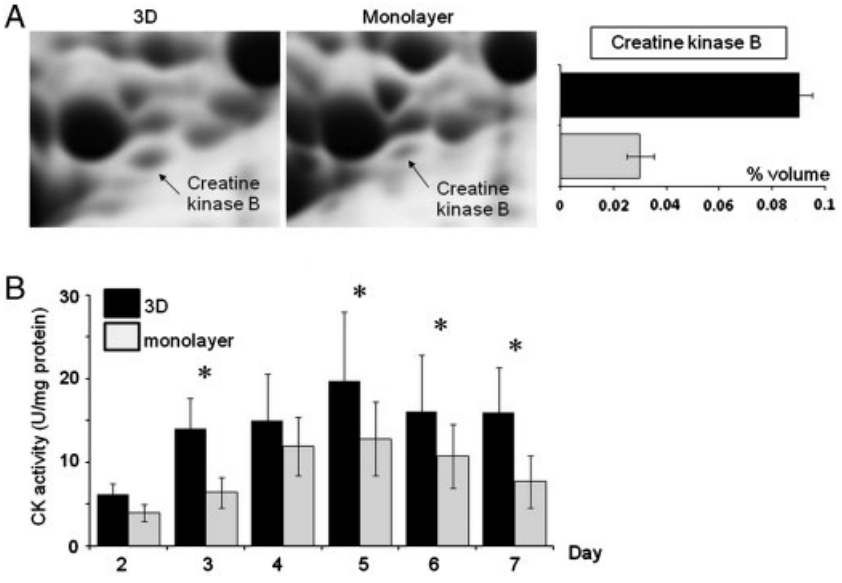

Figure 4. CK expression and activity in 3-D and monolayer culture. (A) CK B in magnified regions of 2-DE and quantitative percent volume; (B) CK activity on Days 2–7 shown as mean ± SD ($n = 3$), $^{*}p < 0.05$. Black bar shows 3-D culture and gray bar shows monolayer culture.

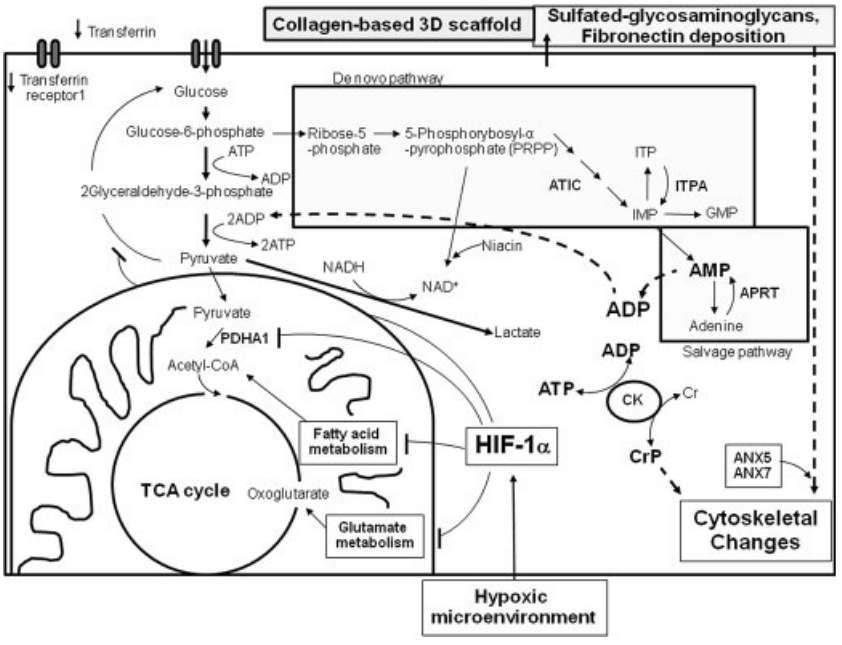

Figure 5. Hypothetical model illustrating possible involvement of altered proteins in metabolic pathways. Dotted arrows indicate hypothetical relationships for changes observed in the 3-D culture system (ANX5 and 7, annexin5 and 7; APRT, adenine phosphoribosyltransferase; ATIC, IMP cyclohydrolase; CK, creatine kinase; Cr, creatine; CrP, creatine phosphate; ITPA, inosine triphosphate pyrophosphatase; PDHA1, pyruvate dehydrogenase1).

4.1 Mitochondrial function deficit and anaerobic glycolysis in 3-D culture

HepG2 in 3-D culture showed upregulation of enzymes involved in anaerobic glycolysis and downregulation of several mitochondrial enzymes involved in oxidative phosphorylation. Occupation of space in the collagen-based scaffold by cell colonies and extracellular content is likely to decrease the ability of oxygen to pass through the 3-D culture, particularly at the central regions. This mimics the rapid growth of the cell populations in small avascular tumors, leading to disturbance of oxygen and nutrient supply in the surrounding environment. Indeed, microenvironmental stress on cancer cells is an important factor leading to metabolic alterations, which mediate angiogenesis, tumor progression and metastasis [3].

Oxygen supply did not appear to be limiting in monolayer culture, since HepG2 in monolayer culture had mitochondrial enzymes for energy production by oxidative phosphorylation, as well as enzymes for fatty acid oxidation, suggesting that glucose oxidation was not the only energy source. In 3-D culture, HepG2 responded to hypoxia by HIF-1α stabilization, which controls the expression of several enzymes involved in mitochondrial function.

Furthermore, HIF-1α enhanced hypoxic glycolytic flux to provide sufficient ATP rapidly for cellular metabolism [18].

4.2 Cellular energy buffer system in 3-D culture

Since HepG2 cells under 3-D culture shift their energy supply from mitochondrial oxidative phosphorylation to anaerobic glycolysis, the creatine kinase/phosphocreatine (CK/PCr) system plays a critical role as an energy buffer. Thus, cells under 3-D culture gradually increased CK activity with time correlating with anaerobic glycolysis. This suggests that ATP from anaerobic glycolysis may be transphosphorylated by CK into PCr to replenish the PCr pool(s) serving as energy supply. CK metabolism also contributes to ATP production in excitable cells and tissues, *e.g.* skeletal muscle, cardiac muscle and spermatozoa [19]. CK is not normally found at high level in liver. Thus CK activity was present at low levels in normal and most pathological human liver samples, but high levels of CK B were found in primary human HCC [20]. Our study is the first to demonstrate that CK/PCr may function as an important energy buffer system in a HCC cell line under the hypoxic microenvironment of 3-D culture.

Nucleotide metabolism is important for tumor growth and is a target for chemotherapy. Enzymes in nucleotide metabolism were upregulated in 3-D culture compared to monolayer culture. Apart from producing DNA building blocks for cellular proliferation, nucleotide metabolism in HepG2 cells in 3-D culture provides another source of cellular chemical energy, as well as coenzyme (NAD^+, nicotinamide adenine dinucleotide) for glycolysis [21]. NAD^+ biosynthesis requires 5-phosphorybosyl-α-pyrophosphatase, niacin and ATP in mammals, so high turnover of the pentose phosphate pathway for 5-phosphorybosyl-α-pyrophosphatase production and high rates of ATP production favor NAD^+ production [22]. This correlates with reports showing that NAD^+ plays a role in energy regulation of cancer cells, and that increased NAD^+ level relates to angiogenesis and tumor progression [23].

4.3 Extracellular matrix deposition in 3-D culture

Histological studies showed that HepG2 culture in 3-D scaffold produced increased levels of sulfated-glycosaminoglycans, an important extracellular matrix constituent, as previously observed [2, 11]. Proteomic studies also showed deposition of fibronectin, absent in monolayer culture. Cells adhere to fibronectin *via* integrins present on the cell surface, and this is one factor leading to tumor progression. Fibronectin and collagen are also external factors enhancing cytoskeletal organization [24, 25]. Deposition of sulfated-glycosaminoglycans and fibronectin changes the microenvironment for HepG2 in 3-D culture, which should affect the cellular characteristics.

4.4 Cytoskeletal changes in 3-D culture

Increased levels of actin, tropomyosin, tubulin (α, β), Rho-GDP dissociation inhibitor, cofilin, profilin and stathmin1 are involved in the coordinated turnover and formation of actin fibers and microtubules [26, 27], so increased expression may contribute to cellular movement [28]. In addition, CK/CrP is an important local ATP-generator for actin-based cytoskeletal organization during cell extension and motility in several cell types, including astrocyte, mesenchymal embryonic fibroblast, phagocytosis and osteoclast [29, 30].

Clathrin and valosin-containing proteins were also upregulated in 3-D culture. Clathrin is involved in sorting and recycling of plasma membrane proteins [31], and forms a complex with valosin-containing proteins for vesicle transport and intracellular trafficking [32]. Upregulation of both proteins may increase the polarization of cells enabling them to perform vectorial functions in absorption and secretion.

4.5 Conclusions

Our findings on the metabolic changes and their relationships are summarized in Fig. 5. 3-D culture appears to create a hypoxic microenvironment, presumably because space between the collagen strands becomes occupied by HepG2 colonies and their extracellular matrix. HepG2 responds to hypoxia mediated by HIF-1α stabilization, leading to decreased expression of several mitochondrial pathways. This includes a shift toward anaerobic glycolysis, with CK/PCr acting as an energy buffer and possibly promoting the cytoskeletal changes observed. 3-D culture showed enhanced sulfated-glycosaminoglycan and fibronectin deposition and upregulation of nucleotide biosynthesis proteins. Changes in proteome pattern of HepG2 in 3-D culture may mimic the development of small avascular HCC *in vivo* before the onset of angiogenesis. Thus, the 3-D culture system appears to be better suited than monolayer culture for studying chemotherapeutic agents and combination strategies, offering a promising direction to fight recurrent tumors after removal of primary lesion.

This work was supported by the Chulabhorn Research Institute and Chulabhorn Graduate Institute, Bangkok, Thailand and the Center of Excellence on Environmental Health, Toxicology and Management of Chemicals, Bangkok, Thailand.

The authors have declared no conflict of interest

5 References

[1] Blum, H. E., Spangenberg, H. C., Hepatocellular carcinoma: an update. *Arch. Iran. Med.* 2007, *10*, 361–371.

[2] Kim, J. B., Three-dimensional tissue culture models in cancer biology. *Semin. Cancer Biol.* 2005, *15*, 365–377.

[3] Bergers, G., Benjamin, L. E., Tumorigenesis and the angiogenic switch. *Nat. Rev. Cancer* 2003, *3*, 401–410.

[4] Kumar, H. R., Zhong, X., Hoelz, D. J., Rescorla, F. J. *et al.*, Three-dimensional neuroblastoma cell culture: proteomic analysis between monolayer and multicellular tumor spheroids. *Pediatr. Surg. Int.* 2008, *24*, 1229–1234.

[5] Chang, T. T., Hughes-Fulford, M., Monolayer and spheroid culture of human liver hepatocellular carcinoma cell line cells demonstrate distinct global gene expression patterns and functional phenotypes. *Tissue Eng. Part A* 2009, *15*, 559–567.

[6] Wu, Y. M., Tang, J., Zhao, P., Chen, Z. N., Jiang, J. L., Morphological changes and molecular expressions of hepatocellular carcinoma cells in three-dimensional culture model. *Exp. Mol. Pathol.* 2009, *87*, 133–140.

[7] Howard, D., Buttery, L. D., Shakesheff, K. M., Roberts, S. J., Tissue engineering: strategies, stem cells and scaffolds. *J. Anat.* 2008, *213*, 66–72.

[8] Gaedtke, L., Thoenes, L., Culmsee, C., Mayer, B., Wagner, E., Proteomic analysis reveals differences in protein expression in spheroid versus monolayer cultures of low-passage colon carcinoma cells. *J. Proteome. Res.* 2007, *6*, 4111–4118.

[9] Grun, B., Benjamin, E., Sinclair, J., Timms, J. F. *et al.*, Three-dimensional *in vitro* cell biology models of ovarian and endometrial cancer. *Cell. Prolif.* 2009, *42*, 219–228.

[10] Sarkar, M. R., Augat, P., Shefelbine, S. J., Schorlemmer, S. *et al.*, Bone formation in a long bone defect model using a platelet-rich plasma-loaded collagen scaffold. *Biomaterials* 2006, *27*, 1817–1823.

[11] Pruksakorn, D., Khamwaen, N., Pothacharoen, P., Arpornchayanon, O. *et al.*, Chondrogenic properties of primary human chondrocytes culture in hyaluronic acid treated gelatin scaffold. *J. Med. Assoc. Thai.* 2009, *92*, 483–490.

[12] Martinez, E. C., Wang, J., Gan, S. U., Singh, R. *et al.*, Ascorbic acid improves embryonic cardiomyoblast cell survival and promotes vascularization in potential myocardial grafts *in vivo*. *Tissue Eng. Part A 16*, 1349–1361.

[13] Ahn, S. J., Costa, J., Emanuel, J. R., PicoGreen quantitation of DNA: effective evaluation of samples pre- or post-PCR. *Nucleic Acids Res.* 1996, *24*, 2623–2625.

[14] Vistica, D. T., Skehan, P., Scudiero, D., Monks, A. *et al.*, Tetrazolium-based assays for cellular viability: a critical examination of selected parameters affecting formazan production. *Cancer Res.* 1991, *51*, 2515–2520.

[15] Bishop, C., Chu, T. M., Shihabi, Z. K., Single stable reagent for creatine kinase assay. *Clin. Chem.* 1971, *17*, 548–550.

[16] Srisomsap, C., Sawangareetrakul, P., Subhasitanont, P., Panichakul, T. *et al.*, Proteomic analysis of cholangiocarcinoma cell line. *Proteomics* 2004, *4*, 1135–1144.

[17] Bradford, M. M., A rapid and sensitive method for the quantitation of microgram quantities of protein utilizing the principle of protein–dye binding. *Anal. Biochem.* 1976, *72*, 248–254.

[18] Young, C. D., Anderson, S. M., Sugar and fat – that's where it's at: metabolic changes in tumors. *Breast Cancer Res.* 2008, *10*, 202.

[19] Wallimann, T., Wyss, M., Brdiczka, D., Nicolay, K., Eppenberger, H. M., Intracellular compartmentation, structure and function of creatine kinase isoenzymes in tissues with high and fluctuating energy demands: the 'phosphocreatine circuit' for cellular energy homeostasis. *Biochem. J.* 1992, *281*(*Pt 1*), 21–40.

[20] Meffert, G., Gellerich, F. N., Margreiter, R., Wyss, M., Elevated creatine kinase activity in primary hepatocellular carcinoma. *BMC Gastroenterol.* 2005, *5*, 9.

[21] Hsu, C. P., Oka, S., Shao, D., Hariharan, N., Sadoshima, J., Nicotinamide phosphoribosyltransferase regulates cell survival through NAD+ synthesis in cardiac myocytes. *Circ. Res.* 2009, *105*, 481–491.

[22] Revollo, J. R., Grimm, A. A., Imai, S., The NAD biosynthesis pathway mediated by nicotinamide phosphoribosyltransferase regulates Sir2 activity in mammalian cells. *J. Biol. Chem.* 2004, *279*, 50754–50763.

[23] Garten, A., Petzold, S., Korner, A., Imai, S., Kiess, W., Nampt: linking NAD biology, metabolism and cancer. *Trends Endocrinol. Metab.* 2009, *20*, 130–138.

[24] Gugutkov, D., Gonzalez-Garcia, C., Rodriguez Hernandez, J. C., Altankov, G., Salmeron-Sanchez, M., Biological activity of the substrate-induced fibronectin network: insight into the third dimension through electrospun fibers. *Langmuir* 2009, *25*, 10893–10900.

[25] Connelly, J. T., Garcia, A. J., Levenston, M. E., Interactions between integrin ligand density and cytoskeletal integrity regulate BMSC chondrogenesis. *J. Cell Physiol.* 2008, *217*, 145–154.

[26] Machesky, L. M., Hall, A., Role of actin polymerization and adhesion to extracellular matrix in Rac- and Rho-induced cytoskeletal reorganization. *J. Cell Biol.* 1997, *138*, 913–926.

[27] Santos, M. F., McCormack, S. A., Guo, Z., Okolicany, J. *et al.*, Rho proteins play a critical role in cell migration during the early phase of mucosal restitution. *J. Clin. Invest.* 1997, *100*, 216–225.

[28] Olk, S., Zoidl, G., Dermietzel, R., Connexins, cell motility, and the cytoskeleton. *Cell Motil. Cytoskeleton* 2009, *66*, 1000–1016.

[29] Kuiper, J. W., van Horssen, R., Oerlemans, F., Peters, W. *et al.*, Local ATP generation by brain-type creatine kinase (CK-B) facilitates cell motility. *PLoS One* 2009, *4*, e5030.

[30] Kuiper, J. W., Pluk, H., Oerlemans, F., van Leeuwen, F. N. *et al.*, Creatine kinase-mediated ATP supply fuels actin-based events in phagocytosis. *PLoS Biol.* 2008, *6*, e51.

[31] Deborde, S., Perret, E., Gravotta, D., Deora, A. *et al.*, Clathrin is a key regulator of basolateral polarity. *Nature* 2008, *452*, 719–723.

[32] Pleasure, I. T., Black, M. M., Keen, J. H., Valosin-containing protein, VCP, is a ubiquitous clathrin-binding protein. *Nature* 1993, *365*, 459–462.

